THE JOURNAL OF BIOLOGICAL CHEMISTRY VOL. 284, NO. 17, pp. 11738–11747, April 24, 2009


# ADAM10, the Rate-limiting Protease of Regulated Intramembrane Proteolysis of Notch and Other Proteins, Is Processed by ADAMS-9, ADAMS-15, and the γ-Secretase*[S]

Received for publication, July 31, 2008, and in revised form, February 10, 2009 Published, JBC Papers in Press, February 11, 2009, DOI 10.1074/jbc.M805894200

**Thomas Tousseyn[‡§1], Amantha Thathiah[‡§2], Ellen Jorissen[‡§2,3], Tim Raemaekers[‡§¶4], Uwe Konietzko[‖], Karina Reiss[**], Elke Maes[‡§], An Snellinx[‡§], Lutgarde Serneels[‡§], Omar Nyabi[‡§], Wim Annaert[‡§¶], Paul Saftig[**], Dieter Hartmann[‡§‡‡5,6], and Bart De Strooper[‡§6,7]**

*From the [‡]Center for Human Genetics, Katholieke Universiteit Leuven (K. U. Leuven), [§]Department for Developmental and Molecular Genetics, and [¶]Laboratory of Membrane Trafficking, Vlaams Instituut voor Biotechnologie (VIB), K. U. Leuven, Herestraat 49, B-3000 Leuven, Belgium, the [**]Department for Biochemistry, Christian-Albrechts-Universität zu Kiel, Otto-Hahn-Platz 9, D-24098 Kiel, Germany, the [‖]Division of Psychiatry Research, University of Zurich, August Forel-Str. 1, 8008 Zurich, Switzerland, and the [‡‡]Anatomisches Institut der Universität Bonn, Nussallee 10, D 53115 Bonn, Germany*

**ADAM10 is involved in the proteolytic processing and shedding of proteins such as the amyloid precursor protein (APP), cadherins, and the Notch receptors, thereby initiating the regulated intramembrane proteolysis (RIP) of these proteins. Here, we demonstrate that the sheddase ADAM10 is also subject to RIP. We identify ADAM9 and -15 as the proteases responsible for releasing the ADAM10 ectodomain, and Presenilin/γ-Secretase as the protease responsible for the release of the ADAM10 intracellular domain (ICD). This domain then translocates to the nucleus and localizes to nuclear speckles, thought to be involved in gene regulation. Thus, ADAM10 performs a dual role in cells, as a metalloprotease when it is membrane-bound, and as a potential signaling protein once cleaved by ADAM9/15 and the γ-Secretase.**

ADAMs[8] (A disintegrin and metalloprotease) are type 1 transmembrane proteins related to snake venom integrin ligands and metalloproteases. All 38 different family members feature a common modular ectodomain structure (1–4) (Fig. 1*A*). In addition to the membrane-bound, full-length prototype, soluble ADAM variants have also been identified, consisting of only the ectodomain or fragments thereof that are released into the intercellular space. Such variants are generated by partial gene duplication (ADAM9) (5), alternative splicing (ADAM12) (6, 7), or proteolysis (ADAMs 8, 13, and 19) (8–10). ADAMs can be grouped either by their tissue distribution and/or functional properties. One major group (ADAMs 2, 3, 5, 6, 16, 18, 20, 21, 24, 25, 26, 29, and 30) is expressed exclusively in the male gonad, with an emerging role in sperm maturation. A second group (ADAMs 2, 7, 11, 18, 22, 23, and 29) is characterized by an inactive protease domain, and they seem to be mainly important for cell adhesion and fusion. A large third group of ADAMs displays a broad expression profile and has demonstrated (ADAMs 8, 9, 10, 12, 17, 19, and 28) or predicted (ADAMs 15, 20, 21, 30, and 33) proteolytic activity. These proteases play a major role in the ectodomain shedding of proteins involved in paracrine signaling, cell adhesion, and intracellular signaling (reviewed in Refs. 11 and 12). The site specificity of the cleavage of these substrates is rather relaxed, and apparently different family members can mutually compensate for each other. This has been illustrated particularly well for the amyloid precursor protein (APP) (13–17).

ADAM10 is one of the proteolytically active ADAM members (15, 18–21). The list of ADAM10 substrates is still growing, confirming the central role of ADAM10 in many important biological processes, such as cell migration and axonal navigation (robo receptors and ephrins (22, 23), cell adhesion (cadherins (19, 21), CD44 and L1 (24)), and regulation of immune reactions, and control of apoptosis (FasL) (25). Importantly, genetic ablation of ADAM10 in vertebrates (15) and invertebrates (26–29) mainly results in loss of Notch phenotypes, indicating the crucial role for this protease in the Notch signaling pathway (30, 31). Finally, ADAM10 is emerging as a major player in human disease. It is up-regulated in several tumors (32), and it is also considered to be protective in Alzheimer disease as it is one of the major α-secretases, cleaving APP within the amyloid-β (Aβ) peptide sequence, which thus pre-

* This work was supported in part by grants from the Alzheimer's Association and the Fonds voor Wetenschappelijk Onderzoek (F.W.O.) (to D. H.), a Stichting Alzheimer Onderzoek-Fondation sur la Recherche sur la Maladie d'Alzheimer-2006 grant (to W. A.), the Deutsche Forschungsgemeinschaft SFB415-TPB9 (to P. S. and K. R.), and a Freedom to Discover grant from Bristol Myers Squib, a Methusalem grant of the Flemish Government (to B. D. S.), and grants from the F.W.O., K.U. Leuven (to G. O. A.), VIB, and Federal Office for Scientific Affairs (IUAP P6/43/), Belgium (to W. A. and B. D. S.).

[S] The on-line version of this article (available at http://www.jbc.org) contains supplemental Fig. S1.

[1] Fellow of the Fund for Scientific Research, Flanders (F.W.O.) and the Belgian American Educational Foundation.

[2] Both authors contributed equally to this work.

[3] Fellow of the Instituut voor de aanmoediging van Innovatie door wetenschap en technologie in Vlaanderen.

[4] Postdoc fellow of the F.W.O.

[5] To whom correspondence may be addressed: Anatomisches Institut der Universität Bonn, Nussallee 10, D 53115 Bonn, Germany. Tel.: 0049-228-73-7684; Fax: 0049-228-73-5905; E-mail: dhartman@uni-bonn.de.

[6] These authors contributed equally to this work.

[7] To whom correspondence may be addressed: Center for Human Genetics, K.U. Leuven and VIB, Campus Gasthuisberg, Herestraat 49, B-3000 Leuven, Belgium. Tel.: 0032-16-346227; Fax: 0032-16-347181; E-mail: Bart.destrooper@med.kuleuven.be.

[8] The abbreviations used are: ADAM, A disintegrin and metalloprotease; ICD, intracellular domains; APP, amyloid precursor protein; CTF, C-terminal fragment; PS, presenilin; WT, wild type; PML, promyelocytic leukemia; MEF, mouse embryonic fibroblast; RIP, regulated intramembrane proteolysis.

cludes amyloid plaque formation (13, 18, 20, 33). Interestingly, two other ADAMs (9 and 17) have also demonstrated α-secretase activity *in vitro* (13, 14, 16, 18). Thus, stimulating α-secretase cleavage is an interesting therapeutic option for Alzheimer disease (20).

A fascinating aspect of ADAM10-mediated proteolysis is the initiation of regulated intramembrane proteolysis (RIP), which is characterized by two consecutive cleavage steps. First, the ectodomain is shed to generate a soluble ectodomain (11, 34). Then, the remaining transmembrane C-terminal fragment (CTFs) becomes a substrate for intramembrane cleaving proteases such as Presenilin/γ-Secretase (35). The fragments generated by this cleavage are released both externally and internally from the membrane and are, in many instances, involved in cell signaling pathways. Notch signaling has been particularly well investigated and it is well known that the Notch intracellular domain, upon release by Presenilin/γ-Secretase, translocates to the cell nucleus and regulates transcription of a series of Notch target genes in so-called transcription factories (36–41).

Presenilin (PS), an aspartyl protease, is the catalytic subunit of the γ-Secretase complex (42, 43). Two different genes encode PS1 and PS2, respectively, which each integrate into different γ-Secretase complexes (44). Although many γ-Secretase substrates have been discovered (reviewed by Kopan (35)), the extent to which the released intracellular domain fragments are important for signaling is not completely clear as most of the work is based on *in vitro* experiments. Thus, the possibility exists that, in many cases, the γ-Secretase could act as an "intramembrane proteasome," removing residual transmembrane protein fragments that were generated by for instance, ectodomain shedding mediated by ADAM members, to avoid creating a bottleneck in the plasma membrane (35).

Here we demonstrate the surprising finding that ADAM10, apart from its central role in protein shedding and the initiation of regulated intramembrane proteolysis of several substrates, is itself subject to a similar proteolytic cascade. This suggests that ADAM10 has, in addition to its important function as a membrane-tethered sheddase, also the potential to be a signal transducing protein itself.

## EXPERIMENTAL PROCEDURES

*Animals, Cell Cultures, and Tissues*—Mice and derived cell lines and the technique used for their derivation and maintenance were as published (17, 45, 46). Primary murine glial and cortical neuronal cultures were established from brains of embryonic day 14.5 mice, as described previously (47).

*cDNA Constructs*—Full-length murine *ADAM9* and *ADAM15* as well as *ADAM9EA* and *ADAM15EA* catalytically inactive mutant constructs were kind gifts from C. P. Blobel (48, 49). *ADAM10* cDNA (complete cds of GenBank™ sequence AF011379) was obtained by PCR from a murine 129/SvJ cDNA library and was recloned into a modified PSG5 expression vector (Stratagene). A VP16-Gal4 sequence (50) was subcloned into *mADAM10* cDNA after introduction of an HpaI restriction site in the *ADAM10* C terminus via site-directed mutagenesis (Stratagene) at positions G745V,H746N. A *mADAM10* construct lacking the ectodomain (containing a signal peptide sequence (amino acids 1–19) joined to amino acids 669–749) was FLAG-tagged (CTTGTCATCGTCGTCCTTGTAGTC) before the stop codon at the C terminus. The PCR product was ligated into a pcDNA3.1 vector (ADAM10ΔE-flag). All constructs were sequenced and contained no errors. For COS and HEK293 cell transfections we used FuGENE 6 (Roche) or Genejuice (Merck Biosciences), according to the manufacturer's protocol.

*Sample Preparation*—Cell extracts were obtained as described before (15). Phenanthroline was added to the protease inhibitor mixture to prevent autocleavage during the extraction procedure, as previously described for TACE (51). The γ-Secretase inhibitor X (carbamic acid tert-butyl ester L-685,458, Calbiochem) was used at 0.1 μM in medium with 2% fetal calf serum, unless otherwise specified (52). Membrane extracts and whole protein extracts were prepared as described previously (53).

*Shedding Assay*—After 24 h of serum starvation (53) culture medium was replaced with fresh serum-free medium containing one of the following protease inhibitors (Calbiochem): TAPI-1 (25 μM), TAPI-2 (25 μM), GM6001 (50 μM), or the appropriate vehicle control. Following 24 h incubation cell viability was checked, cell extracts were obtained, and cell culture supernatants were concentrated ×20 by ultrafiltration (Centricon-10/Millipore).

*α-Secretase Fluorescence Resonance Energy Transfer Assay*—Cell extracts and concentrated supernatant of *ADAM10*$^{-/-}$ and WT MEFs, after overnight conditioning in serum-free medium, were incubated with a fluorogenic substrate peptide mimicking the APP α-secretase cleavage site as indicated by the manufacturer (R&D Systems). Fluorogenic emission was measured by Victor2 (PerkinElmer Life Sciences) at 495 nm.

*Subcellular Fractionation*—Postnuclear supernatants were prepared using a sucrose step gradient protocol (adapted from Fleischer and Kervina (54)). Pooled cells from five 10-cm culture dishes, after 1.5 h treatment with 20 ng/ml leptomycin B (Sigma) (52), were harvested and homogenized in ice-cold buffer (20 mM Hepes-NaOH, pH 7.4, 5 mM $MgCl_2$, 0.25 M sucrose with 0.2 M dithiothreitol, protease inhibitors, without EDTA) using a glass Dounce homogenizer (type S). Cell disruption and integrity of nuclei were checked. SHM2.1 (20 mM Hepes-NaOH, pH 7.4, 5 mM $MgCl_2$, 2.1 M sucrose) was added to the homogenate to obtain a final sucrose concentration of 1.5 M and after centrifugation at 29,000 × *g* (TST41), the pellet was resuspended in SHM 0.25 (20 mM Hepes-NaOH, pH 7.4, 5 mM $MgCl_2$, 0.25 M sucrose). Fractions were collected and analyzed by Western blotting.

SDS-PAGE proteins were separated and transferred as described before (15). Primary antibodies (overnight at 4 °C) and horseradish peroxidase-tagged (Dako) secondary antibodies (1 h at room temperature) were applied. ADAM10 was detected using the polyclonal antiserum (B42.1), generated against the 17 C-terminal amino acid residues (15). N-terminal-specific antibody MAB946 (R&D Systems) only detected ADAM10 when sample buffer contained 1 μM *N*-ethylmaleimide (Pierce) instead of β-mercaptoethanol (55). APP fragments,

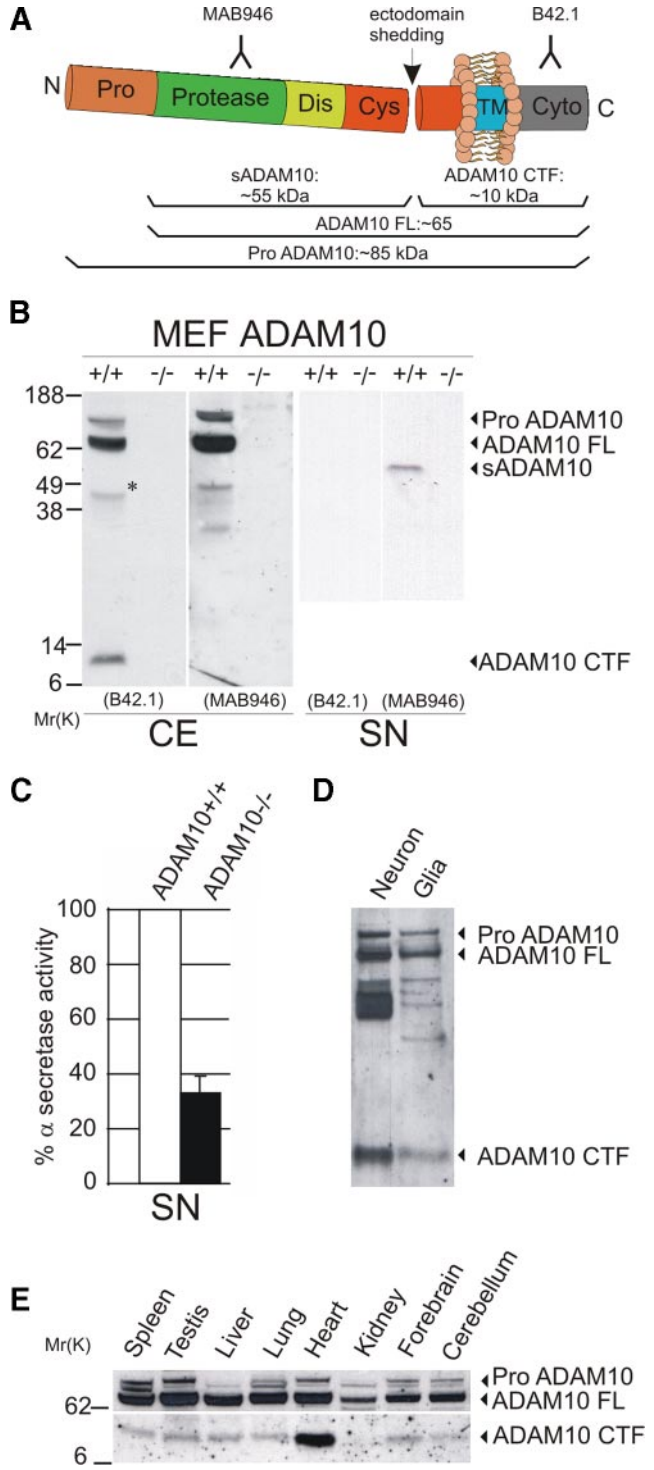


FIGURE 1. **Ectodomain shedding of ADAM10 in MEFs.** *A*, model of the domain organization of ADAM10, which consists of a *pro*-domain (*Pro*) that is proteolytically removed in the trans-Golgi network by pro-protein convertases, a *zinc-binding metalloprotease* (*Protease*) domain, a *disintegrin* domain (*Dis*), which binds to integrin cell adhesion molecules, a *cystein-rich* domain (*Cys*), which can interact with cell surface proteoglycans and in some cases also contains a fusion peptide sequence, a variable *stalk* region, a transmembrane (*TM*) domain, and a cytoplasmic (*Cyto*) domain. Epitopes for C (*B42.1*) and N terminus (*MAB946*) specific antibodies are indicated. Ectodomain shedding (*arrow*) leaves a ~10-kDa membrane-anchored CTF and releases a ~55-kDa soluble ectodomain (*sADAM10*). *B*, Western blot analysis of total wild-type (+/+) MEF cell extracts (*CE*) (50 μg/lane) shows a Pro-ADAM10 (~85 kDa) and a mature ADAM10 (ADAM10 FL, ~65 kDa) after prodomain removal. A third 10-kDa band is detectable (*ADAM10 CTF*) with B42.1, the C-terminal ADAM10 antibody, but not by MAB946, the N-terminal antibody. Additional bands (*asterisk*) are observed in wild-type cells, but not in *ADAM10*-deficient cells. These bands may represent ADAM10 splice variants (see www.genecards.org/cgi-bin/carddisp.pl?gene = ADAM10) or degradation products. A secreted ADAM10 ectodomain (*sADAM10*) is observed in the culture supernatant (*SN*) (30 μg/lane), detected by MAB946, but not B42.1. *C*, SN from WT MEFs was able to cleave a synthetic peptide containing the APP α-secretase cleavage site in a fluorescence resonance energy transfer assay. In MEFs lacking ADAM10 we observed a strong reduction in this cleavage compared with WT. *D*, ADAM10 CTFs are detected by Western blot analysis in cell lysate samples from both neuronal and glial cell cultures (30 μg/lane). *E*, Western blot of total tissue extracts of E16.5 CD1 mouse embryos (50 μg/lane). ADAM10 CTFs were detected to a various extent in all tested organs.

PS1, PS2, and ADAM15 were detected, respectively, using antibodies B63.1, B19.3, B22.4, and SM86-2, as described previously (56, 57). ADAM9 and Sp1 (Santa Cruz) and β-actin (Sigma) were detected by commercial antisera. Blots were developed using the ECL Detection System (Amersham Biosciences) or SuperSignal (Pierce). Signal densities were quantified (in the linear range) with Totallab version 2.01 (GE Healthcare).

*Luciferase Assay*—COS cells were transfected with 200 ng of pFRluc plasmid (Promega) DNA and 200 ng of inducer plasmid DNA: ADAM10-VP16-GAL4, APP-C99-GAL4-VP16, GAL-VP16, or empty vector. The GAL4-VP16 construct without a membrane anchor was used as a γ-Secretase independent positive control. After 24 h, cells were incubated with or without inhibitor X, and after 16 h were lysed and assayed (Victor2; PerkinElmer Life Sciences) (53).

*Confocal Laser Scanning Microscopy*—HEK293 cells transfected with ADAM10ΔE-flag were fixed after 24 h in 1% paraformaldehyde (10 min at room temperature), permeabilized by methanol (−20 °C) or 0.5% Triton X-100/phosphate-buffered saline (5 min), and processed for indirect immunofluorescence (50). Primary antibodies (overnight at 4 °C) and Alexa 488- or 568-conjugated (Molecular Probes, Inc) or Cy3-(shown in red) or Cy2-conjugated (shown in green) (Jackson ImmunoResearch) secondary antibodies (1 h at room temperature) were applied and nuclei were counterstained using Hoechst Bisbenzimid H33342 (Sigma) (10 min at room temperature). Monoclonal M2 and polyclonal anti-FLAG antibodies, as well as antibodies detecting PML, coilin, bromodeoxyuridine, and nucleophosmin/B23 were purchased from Sigma. Antibodies against lamin B and sc-35 were purchased from Santa Cruz and BD Transduction Laboratories, respectively. Coverslips were mounted using Mowiol (Calbiochem). After staining, cells were examined using an inverted microscope (Eclipse E800, Nikon; Plan Apo ×60/1.40 oil) connected to a confocal microscope (Radiance 2100; Zeiss or Leica SP2) and images were acquired using LaserSharp 2000 software. Images were processed in Adobe Photoshop CS. Speckled nuclei were defined as cells containing 3 or more large or 5 or more small granular "speckle-like" structures in their nucleus. 100 FLAG-positive cells were counted manually in a blind fashion to quantify the effect of γ-secretase inhibition (overnight at 37 °C). The number of speckled cells (mean of three experiments) is indicated as a percentage of the amount of ADAM10ΔE-flag-transfected cells.

*Statistical Analysis*—Data were subjected to statistical analysis (one-way analysis of variance with a Bonferroni correction) to determine their significance. $p$ values are demonstrated in the figures using asterisks (*, $p < 0.05$; **, $p < 0.01$; ***, $p < 0.001$).

## RESULTS

*The ADAM10 Ectodomain Is Shed from Fibroblasts in Vitro*—In Western blots of whole cell homogenates, ADAM10 appears as a doublet band of ~85 and 65 kDa, corresponding to the unprocessed pro-form and the mature enzyme, respectively (58). In addition a band at ~10 kDa is observed that reacts exclusively with C terminus-specific antibodies (ADAM10 CTF, Fig. 1, *A* and *B*). It is noteworthy that in some experiments the ADAM10 CTF appears as a doublet band (*e.g.* Fig. 2*B*, *fourth panel*). In the culture supernatant samples of the cells, we also observed a soluble protein at ~55 kDa that was immunoreactive with antibodies against the ADAM10 N terminus but not C terminus (soluble = sADAM10, Fig. 1*B*). These bands were undetectable in cell extracts and supernatants from *ADAM10*$^{-/-}$ MEFs (Fig. 1*B*). Thus, ADAM10 is apparently processed by an unknown protease generating a membrane-bound C-terminal fragment and a secreted, soluble ectodomain. We checked whether the ADAM10 ectofragment shed in the medium retained its proteolytic activity. The supernatant of wild-type MEFs cleaves a synthetic peptide containing the α-secretase cleavage site of APP in a fluorescence resonance energy transfer assay. This activity is strongly reduced in supernatant of MEFs lacking ADAM10 (Fig. 1*C*). In separate experiments we could demonstrate that removal of ADAM10 from the supernatant by immunoprecipitation also reduces significantly proteolytic activity (data not shown).

ADAM10 CTFs were also observed in cell lysates of cultured neurons and astrocytes (Fig. 1*D*) and *in vivo* in brain, liver, lung, heart, and kidney tissue from both embryo (Fig. 1*E*) and adult mice (data not shown). As shown in Fig. 1*E*, considerable differences in ADAM10 processing are observed in different tissues. In particular the heart (which is strongly affected by ADAM10 deficiency, see Ref. 15) displays an abundant accumulation of the ADAM10 CTF.

*ADAM10 Shedding Depends on ADAMs 9 and 15*—To identify the proteases responsible for ADAM10 shedding, we screened wild-type MEF cultures with a panel of inhibitors against all major classes of proteases, but only the metalloprotease inhibitors GM6001, TAPI1, and TAPI2 reduced ADAM10 CTF and sADAM10 accumulation in MEFs, suggesting that the ADAM10 sheddase(s) belong(s) to the metalloprotease family (Fig. 2*A*). Members of the ADAM family are known to be important ectodomain shedding metalloproteases. So far, only 12 of the 38 ADAMs have demonstrated (ADAMs 8, 9, 10, 12, 17, 19, and 28) or predicted (ADAMs 15, 20, 21, 30, and 33) active MP domains. Consequently, we investigated ADAM10 shedding in MEF cell lines deficient in expression of *ADAM*s *9*, *15*, and *19* and cell lines deficient for both *ADAMs 9 and 15*. We found a significant, albeit somewhat variable, reduction in ADAM10 shedding in *ADAM9*-deficient MEF lines (Fig. 2*B*, *fourth* and *seventh panels*, *lanes 4–6*), whereas shedding was virtually abolished in a cell line lacking both *ADAMs 9 and 15* (Fig. 2*B*, *fourth* and *seventh panels*, *lanes 7–9*). No difference in ADAM10 shedding was observed in *ADAM19*$^{-/-}$ MEFs (data not shown). We confirmed that ADAM10 is a novel substrate for ADAM9 and ADAM15 by overexpression experiments in COS cells. Only low amounts of endogenous ADAM10 holoprotein and no CTFs could be detected in untransfected cells (Fig. 2*C*, *first* and *third panels*, *lanes 1* and *2*). However, upon transient overexpression of ADAM10 an intense doublet band of ADAM10 FL as well as ADAM10 CTF and the soluble ADAM10 ectodomain were observed (Fig. 2C, *first* and *third panels*, *lanes 5–7*). When increasing amounts of ADAM9 (0.1 μg in Fig. 2*C*, *second panel*, *lanes 14–15 versus* 1 μg in *lanes 8–10*) were co-overexpressed with ADAM10, more ADAM10 fragments were generated (Fig. 2*C*, *third* and *sixth panels*, *lanes 14–15* and *8–10*, respectively), whereas this effect was undetectable following transfection with similar concentrations of the catalytically inactive *ADAM9EA* mutant (Fig. 2*C*, *lanes 16–17* and *11–13*). A similar increase in sADAM10 was shown when *ADAM15*, but not *ADAM15EA*, was overexpressed in COS cells, demonstrating the ability of ADAM15 to cleave ADAM10 as well. Interestingly, accumulation of the cell-bound ADAM10 CTF was not observed following cleavage by ADAM15 (supplemental Fig. S1), whereas it is a consistent feature of ADAM9-mediated cleavage. Although the precise mechanism is unclear, the observed absence of the ADAM10 CTF following cleavage by ADAM15 cleavage suggests the ADAM10 CTF is rapidly degraded after proteolytic processing by ADAM15.

Finally, we sought to determine whether ADAM9 and -15 are involved in ADAM10 proteolytic processing *in vivo*. Thus, we examined ADAM10 CTF generation in *ADAM9*- and *ADAM9/15*-deficient mouse brain samples from different postnatal ages (Fig. 2*D*). We observed a decrease in ADAM10 CTF generation in the *ADAM9*- and *ADAM9/15*-deficient mouse brain samples relative to WT control samples, demonstrating *in vivo* correlation of the *in vitro* cell culture studies conducted in MEF and COS cell lines. Interestingly, the reduction in ADAM10 CTF generation was less prominent in tissues such as the liver and lung,[9] which suggests the presence of additional tissue-specific ADAM10 sheddases. Apparently, the deficiency of ADAM10 shedding did not result in the accumulation of full-length ADAM10, indicating a tight control of ADAM10 holoprotein levels in the cell.

*ADAM10 CTFs Are Cleaved by γ-Secretase to Release a Free Intracellular Domain*—In many instances, the CTF of type I integral membrane proteins generated by ectodomain shedding are subsequently cleaved by γ-Secretase, a protein complex that contains presenilin as the catalytic subunit. Therefore, we determined whether the ADAM10 CTFs generated by ADAM9 and -15 are also substrates for γ-Secretase (Fig. 3*A*). Inhibiting γ-Secretase activity with the γ-Secretase inhibitor X resulted in an accumulation of ADAM10 CTFs in wild-type cells (Fig. 3*B*). In accordance with this finding, there was a clear accumulation of ADAM10 CTF fragments in *PS1* and *PS1*/*PS2* double deficient MEFs (Fig. 3*C*, *second* and *fourth* or *sixth*

[9] T. Tousseyn, E. Jorissen, D. Hartmann, and B. De Strooper, unpublished observations.

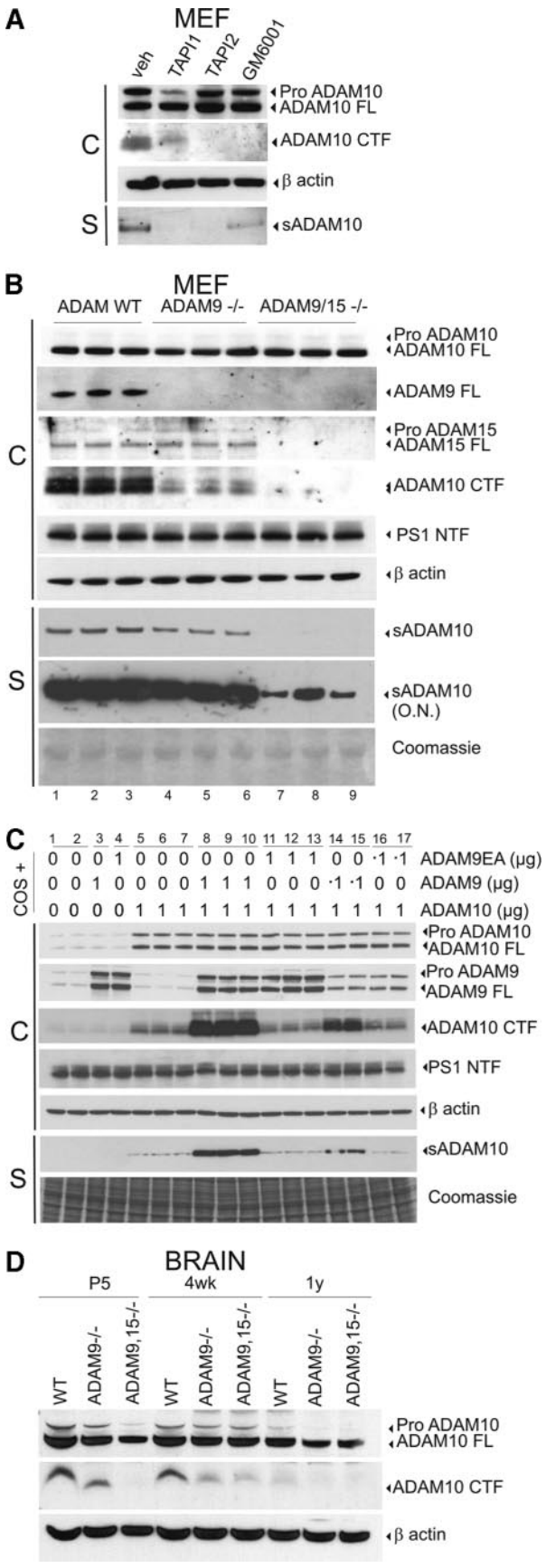


FIGURE 2. **ADAM10 ectodomain shedding is mediated by ADAMs 9 and 15.** *A*, Western blots of total MEF cell extracts (*CE*) (50 μg/lane) and culture supernatants (*SN*) (30 μg/lane). Metalloprotease inhibitors TAPI-1 (25 μM), TAPI-2 (25 μM), and GM6001 (50 μM) significantly reduce ADAM10 processing. *B*, Western blots of total MEF cell extracts and supernatants. Levels of ADAM10 expression are similar in WT, *ADAM9*$^{-/-}$, or *ADAM9/15*$^{-/-}$ cells (*panel 1*). No ADAM9 and ADAM15 protein expression was detected in the respective single and double knockouts (second and *third panels*). Levels of both ADAM10 CTFs and sADAM10 are strongly reduced in *ADAM9*$^{-/-}$ MEFs (*fourth* and *seventh panels*, *lanes 4–6*). Residual ADAM10 CTF accumulation and sADAM10 are strongly reduced in combined *ADAM9/15*$^{-/-}$ MEFs, but not completely abolished as demonstrated by the longer exposure (overnight, *O.N.*) (*fourth* and *seventh panels, lanes 7–9*). Note that the levels of ADAM10 CTFs vary independently of the constant PS1 expression levels (compare *fourth* and *fifth panels*). The ADAM10 CTF appears sometimes as a doublet band, potentially related to post-translational modifications or alternative cleavage sites. *C*, Western blot of total cell extracts and cell supernatant. Untransfected COS cells show the presence of low amounts of endogenously expressed ADAM10 (*first panel*, *lanes 1* and *2*) and ADAM9 (*second panel, lanes 1* and *2*). Overexpression of *ADAM9* alone or *ADAM9EA* does not affect ADAM10 expression (*first panel, lanes 3 and 4,* respectively). In *ADAM10*-transfected cells (1 μg), ADAM10 full-length protein, ADAM10 CTFs, and sADAM10 are easily demonstrated (*third* and *sixth panels, lanes 5–7*). Cotransfection of ADAM10 with increasing amounts of ADAM9 (*second panel*, 0.1 μg in *lanes 14–15* and 1 μg in *lanes 8–10*) causes a parallel increase in ADAM10 CTFs and sADAM10 (*panels 3* and *6, lanes 14–15* and *lanes 8–10*, respectively). This increase was not observed when co-transfecting *ADAM10* with different concentrations of the catalytically inactive *ADAM9EA* mutant (*third* and *sixth panels, lanes 16–17* and *lanes 11–13*). Expression levels of PS1 (*fourth panel*) do not show major variations. The β-actin Western blot and Coomassie stain reflect equal loading of proteins in both cell extract and supernatant samples (*fifth* and *seventh panels,* respectively). *D*, membrane extracts prepared from 5-day-old (*P5*), 4-week-old (*4 wk*), and 1-year-old (*1y*) mice brains show a decrease in ADAM10-CTF formation in ADAM9 and ADAM9/15 knockouts, compared with age-matched WT mice.

*lanes*). Interestingly, the pattern of ADAM10 CTF accumulation in these cell lines is very similar to the CTF accumulation observed with other γ-Secretase substrates, such as APP and Notch, in agreement with the conclusion that the ADAM10 CTF is a valid substrate for γ-Secretase. Additional studies utilizing genetic rescue experiments with wild-type human *PS1*, but not a *PS1* active site mutant, confirmed that ADAM10 CTF is an authentic γ-Secretase substrate (Fig. 3*C*, *seventh* to *ninth lanes*).

We confirmed the role of the γ-Secretase in ADAM10 CTF turnover *in vivo*, by determining ADAM10 CTF generation in various tissues from *PS1*- and *PS2*-deficient mice. ADAM10 CTF accumulation was established in brain, lung, liver, heart, and kidney from E16.5 *PS1*$^{-/-}$ and *PS2*$^{-/-}$ mice. ADAM10 CTF accumulation was prominent in the brain and lung of *PS1*-deficient mice, whereas ADAM10 CTF accumulation was the highest in the liver of *PS2*$^{-/-}$ mice, exceeding the deficit in ADAM10 CTF processing observed in *PS1*$^{-/-}$ mice (Fig. 3*D*). Intriguingly, the liver displays the highest levels of PS2 expression in wild-type animals (59). Thus, these data strongly suggest the ADAM10 CTF is a substrate for both PS1- and PS2-related γ-Secretases.

To confirm the release of ADAM10 intracellular domains (ICD) from ADAM10 CTFs we introduced a VP16-GAL4 sequence close to the C terminus of the ICD domain (Fig. 3*E*) that would result in activation of transcription from a GAL4 upstream activation sequence (UAS)-luciferase reporter gene after being released from the membrane by γ-Secretase. Transfection of COS cells induced a 10-fold activation of the luciferase reporter (Fig. 3*F*, *white bar* in ADAM10-GAL), which was reduced by the γ-Secretase inhibitor X (*InhX*) to the level of dimethyl sulfoxide controls (Fig. 3*F*, *red bar* in ADAM10-GAL). Moreover, cotransfection with ADAM9 resulted in a ~100-fold

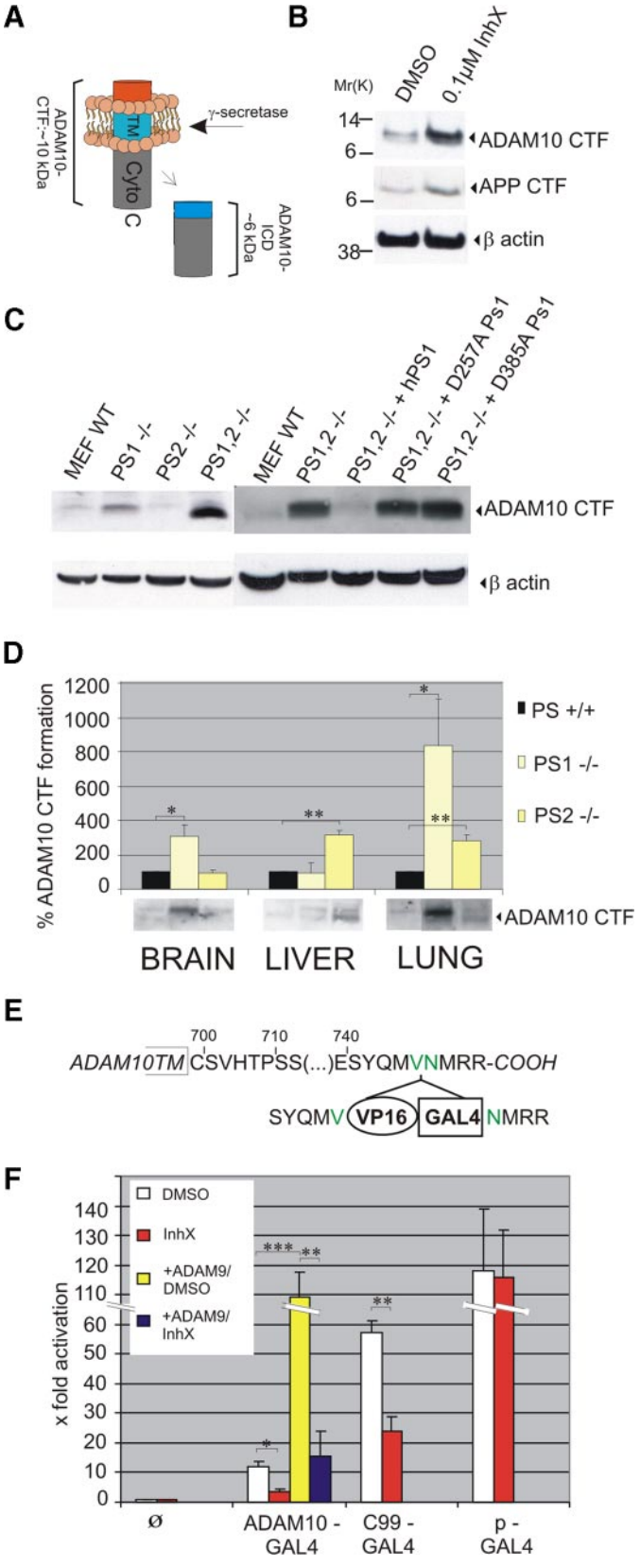


FIGURE 3. **Metabolism of the ADAM10 CTF depends on PS/γ-Secretase activity.** *A*, schematic representation of an ADAM10 CTF generated by ADAM9 or -15 processing. γ-Secretase cleavage of this CTF releases a soluble ICD from the membrane into the cytoplasm. Loss of γ-Secretase activity results in accumulation of the ADAM10 CTF. *B*, Western blots of total cell extracts from MEFs (50 μg/lane) probed with the indicated antibodies. Cells were treated with the γ-Secretase inhibitor InhX (0.1 μM). ADAM10 CTFs and APP CTFs, known γ-Secretase substrates, accumulate in the presence of InhX. *C*, Western blots of *PS1*$^{-/-}$ (*second lane*) and *PS1/2*$^{-/-}$ MEFs (*fourth* and *sixth lanes*) show ADAM10 CTF accumulation. Stable transfection of wild-type human *PS1* (*hPS1*) into *PS1/2*$^{-/-}$ MEFs (*seventh lane*), but not the catalytically inactive *PS1* D257A or D385A mutants, can rescue generation of the ADAM10 CTF (*eighth* and *ninth lanes*). *D*, Western blots of mouse tissue extracts and quantitative analysis of three experiments. ADAM10 CTF accumulation occurs in the *PS1*-deficient brain and lung and *PS2*-deficient liver. *p* values are indicated with asterisks (*, $p < 0.05$; **, $p < 0.01$; ***, $p < 0.001$). *E*, schematic representation of the luciferase reporter construct. A VP16 (activation domain)-GAL4 (binding domain) fusion sequence was cloned to the ADAM10 C terminus. *F*, luciferase assay on COS cells transfected with either empty control vector (ø) or with *ADAM10-VP16-GAL4* or *APP-C99-VP16-GAL4* as positive control. The luciferase reporter, driven by the GAL4 upstream activation sequence, was measured in three experiments and expressed relative to luciferase activation. Transfection of *ADAM10-GAL4* alone resulted in activation of luciferase expression (*white bar*). This effect was inhibited by the γ-Secretase inhibitor X at 0.1 μM (*InhX*, *red bar*). Cotransfection with *ADAM9* (*yellow bar*) strongly stimulated luciferase expression, an effect that could be inhibited by InhX (*blue bar*), demonstrating that the execution of signaling depends on the combined action of ADAM9 and the γ-Secretase. Transfection of *GAL4-VP16* fusion protein (*p*-GAL) directly drives luciferase expression strongly and is independent of γ-Secretase processing (*red bar*, presence of InhX).

reporter activation as a result of the increased generation of the ADAM10 CTF available for processing by the γ-Secretase, effects that were entirely blocked by the γ-Secretase inhibitor X (Fig. 3*F*, *yellow* and *blue bars*, respectively). Thus, these results are consistent with reporter activation initiated by ectodomain cleavage of ADAM10 via ADAM9 and consecutive RIP of the generated ADAM10 CTF by the γ-Secretase resulting in the release of the ADAM10 ICD.

*RIP of ADAM10 Leads to an Intranuclear Accumulation of Its ICD*—Regulated intramembrane proteolysis of several proteins such as the Notch receptor is followed by nuclear translocation of the intracellular domain. Endogenous nuclear ADAM10 immunoreactivity was below detection limits in purified nuclear fractions from MEF cells (Fig. 4, *first lane*), probably reflecting the low nuclear concentrations of the ADAM10 ICD, similar to the Notch receptor ICD (60). However, addition of the nuclear export inhibitor leptomycin B allowed specific detection of a ~4–5-kDa band in nuclear fractions that cross-reacted with ADAM10 C-terminal-specific antibodies (Fig. 4, *second lane*). This band was not observed in nuclei purified from *ADAM10*-deficient cells (Fig. 4, *third lane*) or from cells deficient in *ADAM9* and *-15* or the γ-Secretase components *PS1/2* (Fig. 4, *fourth* and *fifth lanes*, respectively). Interestingly, reintroduction of *hPS1* into PS1/2-deficient cells rescued the appearance of the ADAM10 ICD (Fig. 4, *sixth lane*).

We then confirmed the nuclear localization of the ADAM10 ICD by transfecting HEK293 cells with an ADAM10ΔE-FLAG construct (Fig. 5*A*), which is a membrane-anchored fragment of ADAM10 that requires γ-Secretase processing to release the ICD, but does not require the rate-limiting ectodomain shedding step by ADAM9 or -15. A similar construct has been used previously to study intramembrane proteolysis of Notch. We found that about 30% of the cells transfected with this construct (displaying strong cell surface immunofluorescence when stained with FLAG antibodies), exhibited nuclear immunoreactivity (Fig. 5, *B*, *C*, and *F*, *white bar*). When inhibitor X was used, this percentage dropped to 5% of the FLAG-positive cells, confirming that the γ-Secretase was necessary to release the ADAM10 ICD (Fig. 5, *D–F*, *black bar*). More specifically,

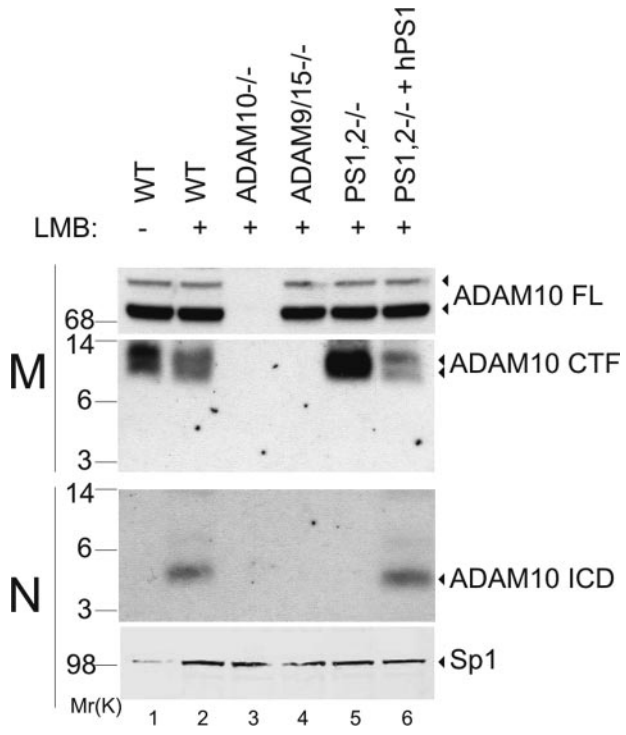


FIGURE 4. **The ADAM10 ICD translocates to the nucleus in MEFs.** Western blots of membrane (*M*) and nuclear (*N*) extracts of the indicated fibroblast cell lines. ADAM10 holoprotein is observed in all lanes except for the *ADAM10*$^{-/-}$ cells (*first panel*). ADAM10 CTFs are present in total cell extracts of WT MEFs, absent in *ADAM10*$^{-/-}$ and in *ADAM9/15*$^{-/-}$ cells, and accumulate in *PS1/2*$^{-/-}$ MEFs (*panel 2*). The ADAM10 ICD could be demonstrated in nuclear fractions of WT cells only after addition of leptomycin B (*LMB*) (100 ng/ml, overnight, *second* to *sixth lanes*) to block nuclear export and is not detectable in *ADAM10*$^{-/-}$, *ADAM9/15*$^{-/-}$, or *PS1/2*$^{-/-}$ cells (*third panel*). Reconstitution of *PS1/2*$^{-/-}$ cells with *hPS1* (*sixth lane*) restores ADAM10 ICD generation and detection in the nucleus. Enrichment of Sp1 confirms the efficiency of LMB treatment (*fourth panel*).

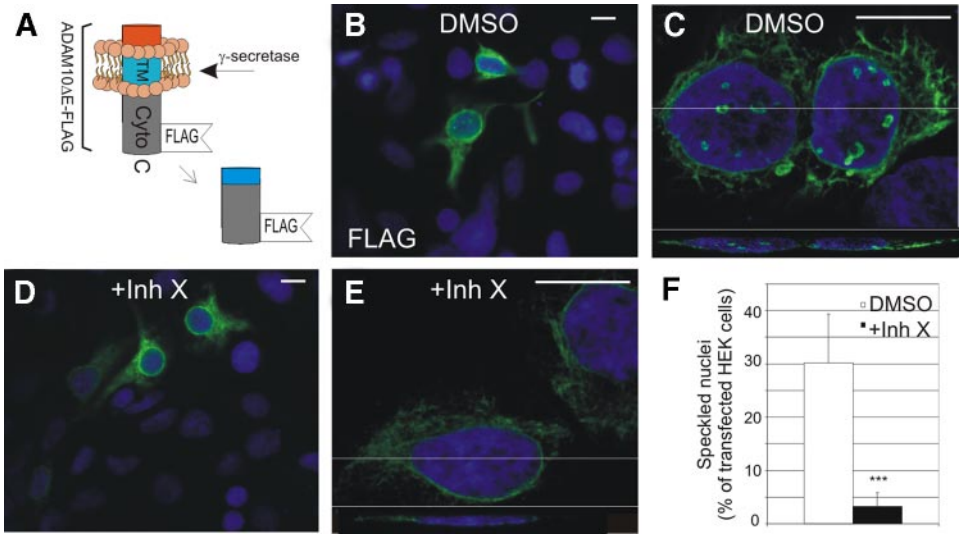


FIGURE 5. **The ADAM10 ICD translocates to the nucleus in HEK293 cells transfected with *ADAM10ΔE-FLAG*.** *A*, a schematic representation of the *ADAM10ΔE-FLAG* construct with release of ADAM10-ICD-FLAG to the nucleus following γ-Secretase cleavage. *B–D*, immunofluorescence labeling of transfected HEK cells using anti-FLAG primary and green fluorescent secondary antibodies (Alexa 488-conjugated). FLAG immunoreactivity (*green*) was observed in the nuclei of about 30% of transfected cells (*B* and *C*). Notice the multipunctate staining pattern resembling that of nuclear speckles (*C*). Cross-section through a speckle at the position of the *white line*, shown in the *inset* in *C*, confirms the intranuclear presence of speckles. Less than 5% of transfected cells show nuclear staining in the presence of the γ-Secretase inhibitor (*InhX*, 0.1 μM) (*D* and *E*). Hoechst nuclear counterstain is in *blue*. *Bar*, 10 μm. *F*, the number of speckled nuclei in the presence or absence of InhX (*white bar*, dimethyl sulfoxide (*DMSO*) control; *black bar*, +InhX) is represented by a bar graph relative to the number of transfected cells (means of three experiments). ***, *p* value <0.001.

ADAM10 ICD immunoreactivity was visible in multiple intense spots in the nucleus (Fig. 5, *B* and *C*), independent of nucleoli, nuclear envelope indentations, and heterochromatin accumulations, as is shown by the respective B23, lamin B, and bromodeoxyuridine immunostainings (Fig. 6, *D–L*). A fraction of the ADAM10 ICD speckle-like structures appear to be closely associated with two known nuclear speckle subtypes, Cajal bodies and PML bodies, as identified by immunoreactivity for p80/coilin and PML, respectively (Fig. 6, *M–R*), but not with sc-35 speckles (Fig. 6, *A–C*). Notably, both Cajal bodies and PML bodies have been shown to localize to actively transcribed gene loci, indirectly supporting a role for ADAM10 in gene transcription control (61, 62).

## DISCUSSION

ADAM10 functions as a membrane-tethered protease, initiating the RIP of proteins such as the Cadherins, the Notch receptor and its ligands, and cytokine receptors. We demonstrate here that ADAM10 is not only executor of, but also subject to, regulated intramembrane proteolysis, being shed by related metalloproteases and subsequently cleaved by γ-Secretase.

We identified two ADAM proteases, *i.e.* ADAM9 and ADAM15, as sheddases responsible for ectodomain cleavage of ADAM10. To date, ADAM9 has been reported to cleave heparin binding-epidermal growth factor and APP *in vitro*; however, ADAM9 knock-out mice display no deficiency in shedding of these proteins (17). In view of studies that suggest that members of the ADAM family can compensate for the absence of one or more family members (13–17), it is usually very difficult to precisely define the function of individual ADAMs, such as ADAM9. Nevertheless, given the reduced accumulation of the ADAM10 CTF *in vivo* in brains of *ADAM9*- and *ADAM9/15*-deficient mice and the *in vitro* evidence in MEF and COS cell lines, ADAM10 appears to be an authentic ADAM9 substrate. We demonstrate here that ADAM15, using the same criteria, is also a putative ADAM10 sheddase. Although ADAM9 and -15 seem to be important ADAM10 sheddases, tissue blots from compound *ADAM9/15* knock-out animals, suggest that at least one other unidentified protease can cleave ADAM10 in its ectodomain in certain tissues. Importantly, ADAM10 is the first identified substrate for ADAM15, which has until now mainly been studied in the context of cell-cell interaction and cell migration, functions that are mediated by its disintegrin and cysteine-rich domains (57, 63, 64).

ADAM10 shedding results in the release of a proteolytically active

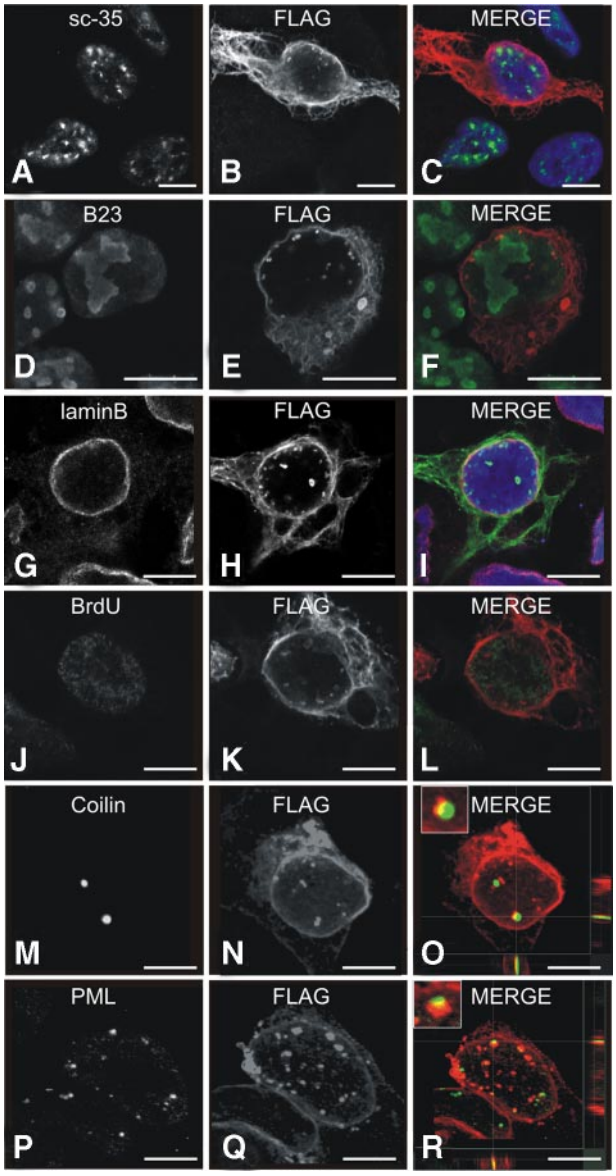


FIGURE 6. **The ADAM10 ICD is localized to a nuclear speckle compartment but is not associated with sc-35, B23, lamin B, or bromodeoxyuridine.** *ADAM10ΔE-FLAG* transfected HEK293 cells were fixed, and nuclear localization of the FLAG-tagged ADAM10 ICD (*B*, *E*, *H*, *K*, *N*, and *Q*) was compared with established marker proteins of speckles (sc-23 in *A*), nucleoli (B23/nucleophosmin in *D*), nuclear membrane (lamin B in *G*), heterochromatin accumulations (bromodeoxyuridine (*BrdU*) in *J*), p80/coilin-positive Cajal bodies (Coilin in *M*), and PML bodies (PML in *P*). Immunodetection was done as described in the legend to Fig. 5. Nuclear ADAM10 immunoreactivity was mainly concentrated in multiple intense spots that did not colocalize with sc-35 speckles (*merged panel* in *C*), nucleoli (*merged panel* in *F*), nuclear membrane indentations (*merged panel* in *I*), or heterochromatin accumulations (*merged panel* in *L*). A fraction of ADAM10 positive speckles was shown to be closely associated with p80/coilin-positive Cajal bodies (*merged panel* in *O*) and PML bodies (*merged panel* in *R*). *Insets* in *O* and *R* represent enlargements and cross-sections in both X/Y and X/Z planes and confirm the close association of FLAG with coilin and PML, respectively. The *white lines* in *O* and *R* point toward the position of the corresponding vertical sections. Detection of primary antibodies was done with Cy3-, Cy2-, Alexa 546-, and Alexa 488-conjugated goat anti-rabbit or goat anti-mouse secondary antibodies (1/1,000 dilution). *Bar*, 10 $\mu$m.

soluble sADAM10 protease that is then available to function as a soluble protease and an ADAM10 CTF, which is then subject to RIP. Accumulation of the ADAM10 CTF in *PS1*- and to a greater extent in *PS1*/*PS2*-deficient fibroblasts indicates that the ADAM10 CTF is a substrate for γ-Secretase. PS2 deficiency in fibroblasts alone had quantitatively little or no effect, in agreement with the relatively minor contribution of PS2 to γ-Secretase activity in fibroblasts (56, 65). ADAM10 CTF processing was reconstituted by expressing wild-type human PS1 in PS1/PS2 double-deficient MEFs, but not by expressing a catalytically inactive mutant hPS1, in which the catalytic aspartyl residues have been replaced by alanine (46). Treatment with γ-Secretase inhibitor X resulted in ADAM10-CTF accumulation. Finally, the accumulation of ADAM10-CTFs in brain, liver, and lung tissue from $PS1^{-/-}$ and $PS2^{-/-}$ mice *in vivo*, firmly establishes ADAM10 as an authentic γ-Secretase substrate.

To address the physiological significance of the sequential ADAM10 proteolytic processing, one option could obviously be that the intramembrane processing merely serves to remove the transmembrane fragments of ADAM10 after shedding of the soluble ectodomain. However, several indirect arguments suggest the possibility that the intracellular domain of ADAM10 exerts a nuclear function. First, we could demonstrate nuclear enrichment of the ADAM10 ICD following treatment with the nuclear export blocker leptomycin B. We could further demonstrate enhanced nuclear staining when we transfected HEK293 cells with a FLAG-tagged ADAM10 construct with a shortened ectodomain (ADAM10ΔE-FLAG), which bypasses the rate-limiting ectodomain shedding step by ADAM9 or -15 (66). Under these conditions, an intense multipunctate nuclear immunoreactivity for ADAM10 could be observed. Nuclear transport of the ADAM10 ICD was reduced following treatment with γ-Secretase inhibitors, providing additional evidence for RIP of ADAM10.

Finally we demonstrate that within the nucleus, the ADAM10 ICD localizes to a nuclear speckle-like compartment, similar to what has been described for Notch- and APP-ICDs (67). Speckles are interchromatin bodies that concentrate proteins involved in mRNA production, splicing, and maturation. Furthermore, a fraction of these ADAM10 ICD-containing speckle-like structures appears to be closely associated with two known nuclear speckle subtypes, Cajal bodies and PML bodies. Both Cajal bodies and PML bodies are associated with actively transcribed gene loci involved in cell survival control (61, 62), providing further circumstantial evidence for a nuclear function of ADAM10. Recently, translocation and colocalization of an ~60-kDa enzymatically active form of ADAM10 with the androgen receptor in the nuclear fraction of a prostate cancer was observed (68), opening the debate as to how these observations are interrelated with our observations of the 4-kDa ADAM10 nuclear fragment.

We conclude that regulated intramembrane proteolysis of ADAM10 and the nuclear accumulation of ADAM10 ICDs suggests a dual function for ADAM10 as a "disintegrin protease and signaling receptor," which is an intriguing idea as it would suggest that proteases can also function as signaling molecules. Recently, other membrane-tethered proteases such as MT1-MMP (69) and BACE1 (70) have been reported to undergo ectodomain shedding, and it may be speculated

that other membrane proteases may have such dual functions as well.

*Acknowledgments—We thank Dr. C. P. Blobel and G. Weskamp (Hospital for Special Surgery at Weill Medical College of Cornell University, New York) for supplying cell lines, knock-out mice, and cDNA constructs. We thank Dr. Jan Cools, Dr. Sebastien Hébert, and Dr. Eva Mortier (Dept. of Human Genetics, University of Leuven, Belgium), Dr. Ben Sprangers, and Dr. Bart Van Wijmeersch (Laboratory of Experimental Transplantation, University of Leuven, Belgium) for constructive discussion; Jan Verhamme for help with the statistical analysis of the data; and Kathleen Craessaerts for technical assistance.*

## REFERENCES


1. Black, R. A., and White, J. M. (1998) *Curr. Opin. Cell Biol.* **10,** 654–659
2. Moss, M. L., and Lambert, M. H. (2002) *Essays Biochem.* **38,** 141–153
3. Primakoff, P., and Myles, D. G. (2000) *Trends Genet.* **16,** 83–87
4. Wolfsberg, T. G., Primakoff, P., Myles, D. G., and White, J. M. (1995) *J. Cell Biol.* **131,** 275–278
5. Hotoda, N., Koike, H., Sasagawa, N., and Ishiura, S. (2002) *Biochem. Biophys. Res. Commun.* **293,** 800–805
6. Gilpin, B. J., Loechel, F., Mattei, M. G., Engvall, E., Albrechtsen, R., and Wewer, U. M. (1998) *J. Biol. Chem.* **273,** 157–166
7. Shi, Z., Xu, W., Loechel, F., Wewer, U. M., and Murphy, L. J. (2000) *J. Biol. Chem.* **275,** 18574–18580
8. Gaultier, A., Cousin, H., Darribere, T., and Alfandari, D. (2002) *J. Biol. Chem.* **277,** 23336–23344
9. Kang, T., Park, H. I., Suh, Y., Zhao, Y. G., Tschesche, H., and Sang, Q. X. (2002) *J. Biol. Chem.* **277,** 48514–48522
10. Schlomann, U., Wildeboer, D., Webster, A., Antropova, O., Zeuschner, D., Knight, C. G., Docherty, A. J., Lambert, M., Skelton, L., Jockusch, H., and Bartsch, J. W. (2002) *J. Biol. Chem.* **277,** 48210–48219
11. Blobel, C. P. (2005) *Nat. Rev.* **6,** 32–43
12. Tousseyn, T., Jorissen, E., Reiss, K., and Hartmann, D. (2006) *Birth Defects Res. C Embryo Today* **78,** 24–46
13. Asai, M., Hattori, C., Szabo, B., Sasagawa, N., Maruyama, K., Tanuma, S., and Ishiura, S. (2003) *Biochem. Biophys. Res. Commun.* **301,** 231–235
14. Buxbaum, J. D., Liu, K. N., Luo, Y., Slack, J. L., Stocking, K. L., Peschon, J. J., Johnson, R. S., Castner, B. J., Cerretti, D. P., and Black, R. A. (1998) *J. Biol. Chem.* **273,** 27765–27767
15. Hartmann, D., de Strooper, B., Serneels, L., Craessaerts, K., Herreman, A., Annaert, W., Umans, L., Lubke, T., Lena Illert, A., von Figura, K., and Saftig, P. (2002) *Hum. Mol. Genet.* **11,** 2615–2624
16. Koike, H., Tomioka, S., Sorimachi, H., Saido, T. C., Maruyama, K., Okuyama, A., Fujisawa-Sehara, A., Ohno, S., Suzuki, K., and Ishiura, S. (1999) *Biochem. J.* **343,** 371–375
17. Weskamp, G., Cai, H., Brodie, T. A., Higashyama, S., Manova, K., Ludwig, T., and Blobel, C. P. (2002) *Mol. Cell. Biol.* **22,** 1537–1544
18. Lammich, S., Kojro, E., Postina, R., Gilbert, S., Pfeiffer, R., Jasionowski, M., Haass, C., and Fahrenholz, F. (1999) *Proc. Natl. Acad. Sci. U. S. A.* **96,** 3922–3927
19. Maretzky, T., Reiss, K., Ludwig, A., Buchholz, J., Scholz, F., Proksch, E., de Strooper, B., Hartmann, D., and Saftig, P. (2005) *Proc. Natl. Acad. Sci. U. S. A.* **102,** 9182–9187
20. Postina, R., Schroeder, A., Dewachter, I., Bohl, J., Schmitt, U., Kojro, E., Prinzen, C., Endres, K., Hiemke, C., Blessing, M., Flamez, P., Dequenne, A., Godaux, E., van Leuven, F., and Fahrenholz, F. (2004) *J. Clin. Investig.* **113,** 1456–1464
21. Reiss, K., Maretzky, T., Ludwig, A., Tousseyn, T., de Strooper, B., Hartmann, D., and Saftig, P. (2005) *EMBO J.* **24,** 742–752
22. Janes, P. W., Saha, N., Barton, W. A., Kolev, M. V., Wimmer-Kleikamp, S. H., Nievergall, E., Blobel, C. P., Himanen, J. P., Lackmann, M., and Nikolov, D. B. (2005) *Cell* **123,** 291–304
23. Mancia, F., and Shapiro, L. (2005) *Cell* **123,** 185–187
24. Mechtersheimer, S., Gutwein, P., Agmon-Levin, N., Stoeck, A., Oleszewski, M., Riedle, S., Postina, R., Fahrenholz, F., Fogel, M., Lemmon, V., and Altevogt, P. (2001) *J. Cell Biol.* **155,** 661–673
25. Schulte, M., Reiss, K., Lettau, M., Maretzky, T., Ludwig, A., Hartmann, D., de Strooper, B., Janssen, O., and Saftig, P. (2007) *Cell Death & Differ.* **14,** 1040–1049
26. Lieber, T., Kidd, S., and Young, M. W. (2002) *Genes Dev.* **16,** 209–221
27. Pan, D., and Rubin, G. M. (1997) *Cell* **90,** 271–280
28. Sotillos, S., Roch, F., and Campuzano, S. (1997) *Development* (*Camb.*) **124,** 4769–4779
29. Wen, C., Metzstein, M. M., and Greenwald, I. (1997) *Development* (*Camb.*) **124,** 4759–4767
30. Hattori, M., Osterfield, M., and Flanagan, J. G. (2000) *Science* **289,** 1360–1365
31. Rooke, J., Pan, D., Xu, T., and Rubin, G. M. (1996) *Science* **273,** 1227–1231
32. McCulloch, D. R., Akl, P., Samaratunga, H., Herington, A. C., and Odorico, D. M. (2004) *Clin. Cancer Res.* **10,** 314–323
33. Deuss, M., Reiss, K., and Hartmann, D. (2008) *Curr. Alzheimer Res.* **5,** 187–201
34. Sahin, U., Weskamp, G., Kelly, K., Zhou, H. M., Higashiyama, S., Peschon, J., Hartmann, D., Saftig, P., and Blobel, C. P. (2004) *J. Cell Biol.* **164,** 769–779
35. Kopan, R., and Ilagan, M. X. (2004) *Nat. Rev.* **5,** 499–504
36. Brou, C., Logeat, F., Gupta, N., Bessia, C., LeBail, O., Doedens, J. R., Cumano, A., Roux, P., Black, R. A., and Israel, A. (2000) *Mol. Cell* **5,** 207–216
37. De Strooper, B., Annaert, W., Cupers, P., Saftig, P., Craessaerts, K., Mumm, J. S., Schroeter, E. H., Schrijvers, V., Wolfe, M. S., Ray, W. J., Goate, A., and Kopan, R. (1999) *Nature* **398,** 518–522
38. Mumm, J. S., Schroeter, E. H., Saxena, M. T., Griesemer, A., Tian, X., Pan, D. J., Ray, W. J., and Kopan, R. (2000) *Mol. Cell* **5,** 197–206
39. Struhl, G., and Greenwald, I. (1999) *Nature* **398,** 522–525
40. Konietzko, U., Goodger, Z. V., Meyer, M., Kohli, B. M., Bosset, J., Lahiri, D. K., and Nitsch, R. M. (2008) *Neurobiol. Aging*, in press
41. Xu, M., and Cook, P. R. (2008) *J. Cell Biol.* **181,** 615–623
42. De Strooper, B., Saftig, P., Craessaerts, K., Vanderstichele, H., Guhde, G., Annaert, W., Von Figura, K., and Van Leuven, F. (1998) *Nature* **391,** 387–390
43. Wolfe, M. S., Xia, W., Ostaszewski, B. L., Diehl, T. S., Kimberly, W. T., and Selkoe, D. J. (1999) *Nature* **398,** 513–517
44. De Strooper, B. (2003) *Neuron* **38,** 9–12
45. Hartmann, D., Tournoy, J., Saftig, P., Annaert, W., and De Strooper, B. (2001) *J. Mol. Neurosci.* **17,** 171–181
46. Nyabi, O., Bentahir, M., Horre, K., Herreman, A., Gottardi-Littell, N., Van Broeckhoven, C., Merchiers, P., Spittaels, K., Annaert, W., and De Strooper, B. (2003) *J. Biol. Chem.* **278,** 43430–43436
47. Cai, D., Qiu, J., Cao, Z., McAtee, M., Bregman, B. S., and Filbin, M. T. (2001) *J. Neurosci.* **21,** 4731–4739
48. Kratzschmar, J., Lum, L., and Blobel, C. P. (1996) *J. Biol. Chem.* **271,** 4593–4596
49. Weskamp, G., Kratzschmar, J., Reid, M. S., and Blobel, C. P. (1996) *J. Cell Biol.* **132,** 717–726
50. Annaert, W. G., Esselens, C., Baert, V., Boeve, C., Snellings, G., Cupers, P., Craessaerts, K., and De Strooper, B. (2001) *Neuron* **32,** 579–589
51. Schlondorff, J., Becherer, J. D., and Blobel, C. P. (2000) *Biochem. J.* **347,** 131–138
52. Shearman, M. S., Beher, D., Clarke, E. E., Lewis, H. D., Harrison, T., Hunt, P., Nadin, A., Smith, A. L., Stevenson, G., and Castro, J. L. (2000) *Biochemistry* **39,** 8698–8704
53. Serneels, L., Dejaegere, T., Craessaerts, K., Horre, K., Jorissen, E., Tousseyn, T., Hebert, S., Coolen, M., Martens, G., Zwijsen, A., Annaert, W., Hartmann, D., and De Strooper, B. (2005) *Proc. Natl. Acad. Sci. U. S. A.* **102,** 1719–1724
54. Fleischer, S., and Kervina, M. (1974) *Methods Enzymol.* **31,** 6–41
55. Partis, M. D. (1983) *J. Prot. Chem.* **2,** 263–277
56. Herreman, A., Hartmann, D., Annaert, W., Saftig, P., Craessaerts, K., Serneels, L., Umans, L., Schrijvers, V., Checler, F., Vanderstichele, H., Baekelandt, V., Dressel, R., Cupers, P., Huylebroeck, D., Zwijsen, A., Van Leu-

ven, F., and De Strooper, B. (1999) *Proc. Natl. Acad. Sci. U. S. A.* **96,** 11872–11877
57. Horiuchi, K., Weskamp, G., Lum, L., Hammes, H. P., Cai, H., Brodie, T. A., Ludwig, T., Chiusaroli, R., Baron, R., Preissner, K. T., Manova, K., and Blobel, C. P. (2003) *Mol. Cell. Biol.* **23,** 5614–5624
58. Anders, A., Gilbert, S., Garten, W., Postina, R., and Fahrenholz, F. (2001) *FASEB J.* **15,** 1837–1839
59. Donoviel, D. B., Hadjantonakis, A. K., Ikeda, M., Zheng, H., Hyslop, P. S., and Bernstein, A. (1999) *Genes Dev.* **13,** 2801–2810
60. Schroeter, E. H., Kisslinger, J. A., and Kopan, R. (1998) *Nature* **393,** 382–386
61. Cioce, M., and Lamond, A. I. (2005) *Annu. Rev. Cell Dev. Biol.* **21,** 105–131
62. Zimber, A., Nguyen, Q. D., and Gespach, C. (2004) *Cell. Signal.* **16,** 1085–1104
63. Eto, K., Puzon-McLaughlin, W., Sheppard, D., Sehara-Fujisawa, A., Zhang, X. P., and Takada, Y. (2000) *J. Biol. Chem.* **275,** 34922–34930
64. Martin, J., Eynstone, L. V., Davies, M., Williams, J. D., and Steadman, R. (2002) *J. Biol. Chem.* **277,** 33683–33689
65. Schulz, J. G., Annaert, W., Vandekerckhove, J., Zimmermann, P., De Strooper, B., and David, G. (2003) *J. Biol. Chem.* **278,** 48651–48657
66. Struhl, G., and Adachi, A. (2000) *Mol. Cell* **6,** 625–636
67. von Rotz, R. C., Kohli, B. M., Bosset, J., Meier, M., Suzuki, T., Nitsch, R. M., and Konietzko, U. (2004) *J. Cell Sci.* **117,** 4435–4448
68. Arima, T., Enokida, H., Kubo, H., Kagara, I., Matsuda, R., Toki, K., Nishimura, H., Chiyomaru, T., Tatarano, S., Idesako, T., Nishiyama, K., and Nakagawa, M. (2007) *Cancer Sci.* **98,** 1720–1726
69. Osenkowski, P., Toth, M., and Fridman, R. (2004) *J. Cell. Physiol.* **200,** 2–10
70. Benjannet, S., Elagoz, A., Wickham, L., Mamarbachi, M., Munzer, J. S., Basak, A., Lazure, C., Cromlish, J. A., Sisodia, S., Checler, F., Chretien, M., and Seidah, N. G. (2001) *J. Biol. Chem.* **276,** 10879–10887